Article

Cobalt-Catalyzed Regioselective Olefin Isomerization Under Kinetic Control

Xufang Liu, Wei Zhang, Yujie Wang, Ze-Xin Zhang, Lei Jiao, and Qiang Liu

J. Am. Chem. Soc., **Just Accepted Manuscript** • DOI: 10.1021/jacs.8b01815 • Publication Date (Web): 21 May 2018

Cobalt-Catalyzed Regioselective Olefin Isomerization Under Kinetic Control

Xufang Liu, Wei Zhang, Yujie Wang, Ze-Xin Zhang, Lei Jiao* and Qiang Liu*

Center of Basic Molecular Science (CBMS), Department of Chemistry, Tsinghua University, Beijing 100084, China.

ABSTRACT: Olefin isomerization is a significant transformation in organic synthesis, which provides a convenient synthetic route for internal olefins and remote functionalization processes. The selectivity of an olefin isomerization process is often thermodynamically controlled. Thus, to achieve selectivity under kinetic control is very challenging. Herein, we report a novel cobalt-catalyzed regioselective olefin isomerization reaction. By taking the advantage of fine-tunable NNP-pincer ligand structures, this catalytic system features high kinetic control of regioselectivity. This mild catalytic system enables the isomerization of 1,1-disubstituted olefins bearing a wide range of functional groups in excellent yields and regioselectivity. The synthetic utility of this transformation was highlighted by the highly selective preparation of a key intermediate for the total synthesis of minfiensine. Moreover, a new strategy was developed to realize the selective monoisomerization of 1-alkenes to 2-alkenes dictated by installing substituents on the γ-position of the double bonds. Mechanistic studies supported that the *in-situ* generated Co-H species underwent migratory insertion of double bond/β-H elimination sequence to afford the isomerization product. The less hindered olefin products were always preferred in this cobalt-catalyzed olefin isomerization due to an effective ligand control of the regioselectivity for the β-H elimination step.

INTRODUCTION

Olefin isomerization is an atom-economical and synthetically useful transformation.[1] Two prominent features of this reaction are: (1) convenient synthesis of internal olefins via the isomerization of easily accessible terminal alkenes[2] (e.g. introducing an alkenyl group via isomerization of an allyl group); and (2) remote functionalization of the original C=C double bond, which is driven by a thermodynamically favored termination step.[3] As shown in Figure 1a, olefin isomerizations are thermodynamically driven to produce more stable alkene isomers. Although a wide range of efficient olefin isomerization reactions have been developed, the selectivity control of this process is still challenging. When the more stable isomerized olefin is the desired product, it is less problematic due to the easily accessible selectivity under thermodynamic control. For example, the isomerization of alkenyl alcohols to carbonyl compounds is a thermodynamically driven chain-walking process of double bonds (Figure 1b).[3f,3j,4] Thus, as long as the chain walking process is fast and reversible, the most stable carbonyl product will dominate the product distribution. In case the desired isomerization product is not the most stable isomer, to control the regioselectivity becomes rather challenging.[5] A typical example is the selective monoisomerization of 1-alkenes to 2-alkenes (Figure 1c). It is difficult to avoid overisomerization to generate other isomers with similar stability.[6] To achieve the desired selectivity, the catalysts utilized in such reactions should well distinguish the different reactivity between 1-alkenes and 2-alkenes leading to a smaller activation energy barrier $\Delta G^{\neq}_1$ compared with $\Delta G^{\neq}_2$ for over-isomerization. Notably, a number of effective transition-metal catalysts have been developed for this selective monoisomerization process, which represents an attractive route to 2-alkenes from readily available 1-alkenes.[7] From a synthetic point of view, other regioselective olefin isomerizations under kinetic control would also be highly desired because the target products for isomerization reactions may be thermodynamically disfavored compared with other possible isomerized products.

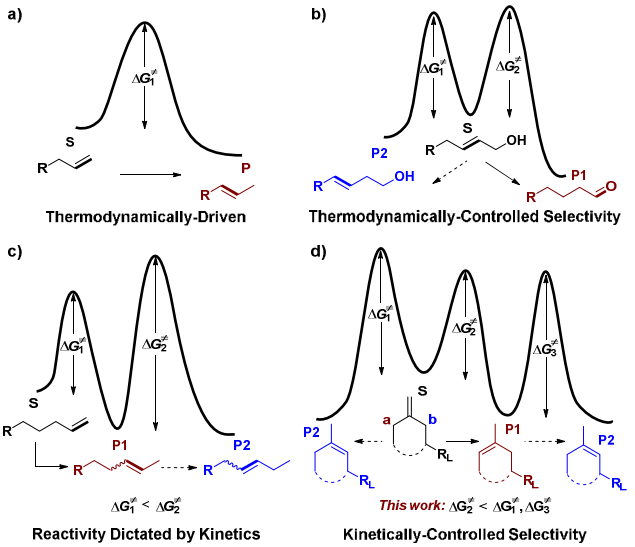

Figure 1. Typical energy profiles for the olefin isomerization reactions.

A representative case is the selective isomerization of 1,1-disubstituted olefins to afford the less hindered double

bond shifted products (Figure 1d). In this case, the double bond migration process of substrate **S** has essentially two unpredictable directions, and the desired product **P1** may further isomerize to the other isomer **P2** with similar stability. As a result, the control of regioselectivity is very demanding. To achieve a high regioselectivity, it is necessary that the catalyst have a means to precisely differentiate the steric hindrance of positions **a** and **b** on the substrate **S**, which will require a kinetically-controlled scenario. In this scenario, the isomerization process ought to be irreversible, and the energy barrier $\Delta G^{\neq}_2$ for the formation of desired isomer **P1** is smaller than both $\Delta G^{\neq}_1$ and $\Delta G^{\neq}_3$. To date this type of olefin isomerization reaction has not been studied in detail, and an efficient catalytic system is still missing from the repertoire that could provide effective kinetic control of regioselectivity for olefin isomerizations.

In fact, such an olefin isomerization is of potential synthetic value, in particular in natural product synthesis. In a recent synthesis of an indole alkaloid nature product, minfiensine, accomplished by one of our groups, the regioselective isomerization of the exocyclic olefin **1a** stood out as a key step for the originally designed late-stage oxidation strategy (Scheme 1).[8] It perfectly represents the reaction scenario in Figure 1d involving two possible reaction sites **a** and **b** with different steric hindrance. However, the undesired regioisomer **3a** was thermodynamically more stable and thus isomerization to **3a** dominated the reaction under classic acidic conditions for olefin isomerization. The lack of efficient olefin isomerization catalysts that could selectively deliver the desired isomer **2a** hampered our original synthetic plan. This showcase example prompted us to systematically study olefin isomerization under kinetic control and therefore to develop an efficient and selective catalytic system based on our experience in the development of pincer cobalt catalysts.[9]

Scheme 1. A Synthetically Useful Olefin Isomerization.

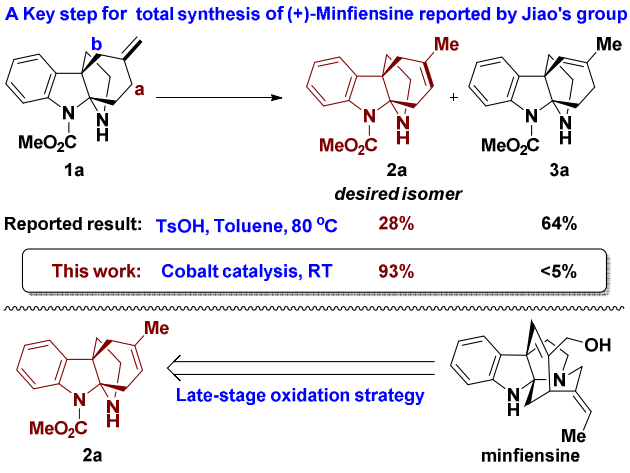

Herein, we report a series of cobalt pincer complexes with well-defined structures as effective catalysts to realize *olefin isomerizations under kinetic control* in excellent regioselectivity. Distinguishing itself from other reported methods for olefin isomerization, this system achieves effective kinetic control of the isomerization process via the repulsion interaction between the bulky substituents on the substrates and the ligand spheres of catalysts. This effect ensures the isomerization occurs only on the less sterically hindered site. The catalytic system works well not only for the regioselective isomerization of 1,1-disubstituted olefins, but also for the selective monoisomerization of terminal olefins with a blocking substituent at the γ-position of the C=C bond. These cobalt-based catalysts enable steric-selective shift of the C=C bond and enrich the selectivity mode of catalytic olefin isomerization.

RESULTS AND DISCUSSION

In the total synthesis of minfinsine, we planned to obtain olefin **2a** by isomerizing exocyclic olefin **1a**. Unfortunately, the major product was undesired regioisomer **3a** under the classic acid promoted olefin isomerization.[8] Independent isomerization experiment of isolated **2a** under identical conditions afforded the same product distribution with a ratio of 1:2.2 for **2a**/**3a** (Eq 1). These results demonstrated that under Brønsted acid-catalyzed conditions, the olefin isomerization is under thermodynamic control, and the desired isomer **2a** is thermodynamically disfavored (DFT calculation confirmed that **2a** is less stable than **3a** by 0.5 kcal/mol in terms of Gibbs free energy). This problem motivated us to develop a kinetically controlled olefin isomerization via cobalt catalysis to access the desired but less stable product **2a** in a high regioselectivity.

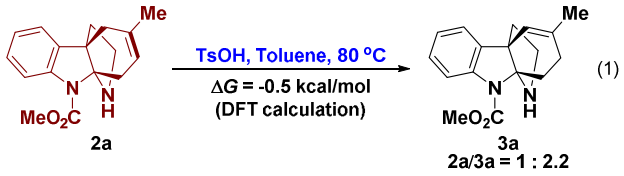

Catalyst Screening

We commenced this study by investigating the catalytic activities of a series of cobalt complexes developed by us[9] in the olefin isomerization of **1a** (Table 1). These reactions were performed in the presence of 1 mol% cobalt catalyst and 10 mol% of ammonia borane as the additive in methanol. Cobalt catalysts **I** and **II** supported by P-tertbutyl and P-isopropyl PNP ligands displayed no reactivity (entries 1 and 2). We envisioned that a modification from PNP to NNP pincer ligands would give rise to hemilabile cobalt catalysts, which may facilitate the isomerization process, owing to the fact that the pyridine coordination site would create a less sterically hindered metal center to promote its interaction with the olefin substrate. Interestingly, these NNP pincer cobalt catalysts **III-VI** indeed exhibited much higher activity (entries 3-6). The P-tertbutyl NNP ligand gave better conversion and yield compared with the results of P-isopropyl and P-phenyl NNP ligands. Moreover, the 5,6 NNP cobalt catalysts **VII** and **VIII** with an enlarged metallacycle were more effective, leading to a higher regioselectivity of **2a** (up to 17:1).

Specifically, 93% isolated yield of **2a** was obtained using cobalt catalyst **VIII** (entry 9). There was no reaction using bulkier *ortho*-Me substituted 5,6 NNP cobalt catalyst **IX**, whereas it shows high reactivity for other more reactive olefin substrates (Scheme 6). A change of counterion of the cobalt complexes from chloride to iodide resulted in similar yield and regioselectivity for **2a** (entry 11). Catalyst with an imine donor, complex **XI**, led to higher regioselectivity but lower conversion compared with the result of the corresponding catalyst **III**, which is supported by an amine ligand (entry 12). *N*-methyl-substituted catalyst **XII** resulted in much lower conversion, albeit with a ratio of **2a**:**3a** up to 23:1. These results revealed the crucial role of catalyst structures in controlling of regioselectivity.

Table 1. Pincer Cobalt Complexes Catalyzed Olefin Isomerization Reaction of **1a**.[a]

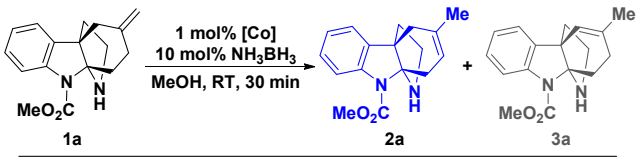

entry	[Co]	conv. **1a** [%]	**2a** : **3a**[b]	yield **2a** [%][c]
1	**I**	0	-	0
2	**II**	0	-	0
3	**III**	98	8 : 1	87
4	**IV**	71	11 : 1	65
5	**V**	30	13 : 1	24
6	**VI**	99	6 : 1	83
7	**VII**	99	8 : 1	88
8	**VIII**	96	17 : 1	90
9[d]	**VIII**	99	17 : 1	93
10	**IX**	0	-	0
11	**X**	91	10 : 1	82
12	**XI**	86	15 : 1	79
13	**XII**	42	23 : 1	39

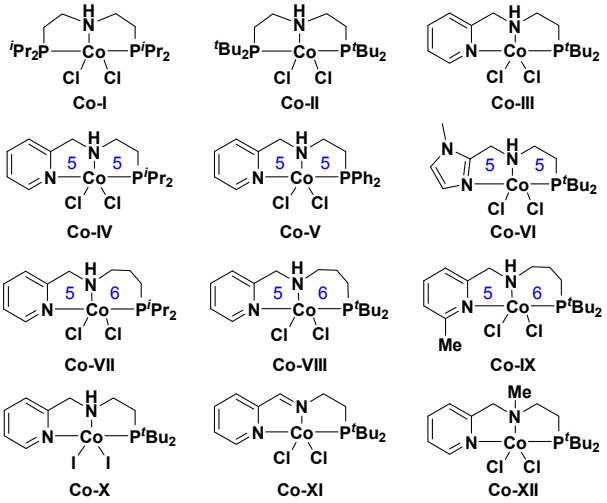

[a]Reaction conditions: **1a** (0.05 mmol), NH_3BH_3 ($5*10^{-3}$ mmol) and Co catalyst ($5*10^{-4}$ mmol) in 0.5 mL of MeOH. [b]The ratio of **2a** : **3a** were determined by ^{1}H NMR. [c]NMR yields. [d]Reaction time was 1 h. Isolated yield was shown.

To make a comparison with other known catalysts for olefin isomerization, we tested 10 reported catalytic systems based on different transition metals, including Pd,[3f,7g] Rh,[2c] Ru,[3j,10] Ir,[4] Fe[2e,7f] and Co[7b,11], for the isomerization reaction of **1a** (Table 2). The optimized reaction conditions reported in the literatures were directly applied without modification.[12] Among these known isomerization catalysts, only the Co(Sal*t*Bu,*t*Bu)Cl/silane catalytic system reported by the Shenvi group[11] was active enough to give high conversion. However, even in that system, only 67% selectivity for **2a** was achieved (entry 9). Other tested catalysts provided much lower conversion and selectivity. This comparison highlighted the unique advantage of our pincer cobalt catalysts for this regioselective olefin isomerization reaction.

Table 2. Performance of Representative Known Catalysis Systems in Olefin Isomerization Reaction of **1a**.[a]

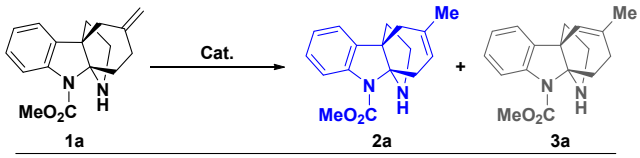

entry	standard conditions	**1a** : **2a** : **3a**	ref.
1	1 mol% $Pd(dba)_2$,1 mol% P(^{t}Bu)$_3$, 1 mol% ^{i}PrCOCl, Toluene, 80 °C, 24 h	100 : 0 : 0	7g
2	5 mol% Mazet's Catalyst, 5.5 mol% $NaBAr_F$, 50 mol% cyclohexene, DCE, 85 °C, 18 h	86 : 8 : 5	3f
3	5 mol% $[Rh(CO)_2Cl]_2$, 12 mol% dppm, DCE, 75 °C, 24 h	100 : 0 : 0	2c
4	5 mol% Crabtree's catalyst, H_2 (1 min) then degassed, THF, RT, 4 h	100 : 0 : 0	4
5	2 mol% Grotjahn's catalyst, Acetone, RT, 15 h	72 : 26 : 3	3j
6	10 mol% Grubbs II catalyst, MeOH, 60 °C, 3 h	100 : 0 : 0	10
7[b]	5 mol% $Fe(acac)_3$, 50 mol% PhMgBr, THF, RT, 15 h	—	2e
8	1 mol% $Fe_3(CO)_{12}$, KOH/H_2O, Diglyme, 80 °C, 15 h	100 : 0 : 0	7f
9	10 mol% Co^{III}(Salen)Cl, 20 mol% $PhSiH_3$, PhH, RT, 24 h	0 : 2 : 1	7b
10	10 mol% $CoBr_2$(BDPP) 20 mol% ZnI_2, 20 mol% Zn 5 mol% Ph_2PH, DCM, RT	100 : 0 : 0	11

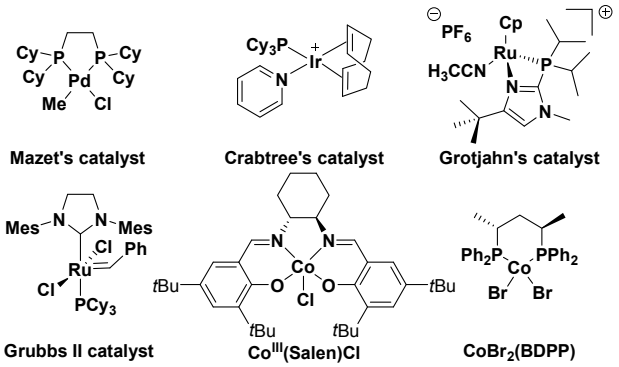

[a]The ratio of **1a** : **2a** : **3a** were determined by ^{1}H NMR. [b]A complicated reaction mixture was generated with full conversion of **1a**.

Substrate Scope

Furthermore, the isomerization of other tetracyclic olefin substrates **1b** and **1c** with different *N*-protecting groups were also investigated under the optimized conditions (Scheme 2). Different *N*-substituents and free amine functionality on the substrates afforded similarly good regioselectivity and yields for the desired less bulky olefin product **2**.

Scheme 2. Co-Catalyzed Regioselective Isomerization of Tetracyclic Olefin 1.[a]

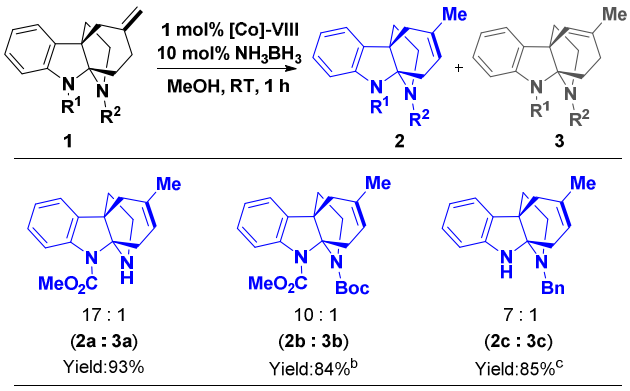

[a]Reaction conditions: 0.05 mmol substrate, 1 mol% **Co-VIII**, 10 mol% H_3NBH_3, 0.5 mL MeOH, at RT for 1 h. Isolated yields of **2** were shown. [b]NMR yield. [c]5 mol% **Co-VIII** was used.

To demonstrate the generality of this regioselective olefin isomerization reaction, we firstly prepared a variety of β-substituted exocyclic olefin substrates **1** with different ring size. The regioselective isomerization of exocyclic olefins **1** were then systematically studied (Scheme 3). Delightfully, the reactions of six-membered ring substrates gave excellent yields of desired olefin products **2** in high regioselectivity (**2d-2m**). It was found that the more sterically hindered substituent on β-position of the double bond gave rise to a larger ratio of **2**:**3** (**2d-2h**). Moreover, a wide range of functional groups including, ester, amide, silyl ether, thio ether, bromo, hydroxyl, and amine, were well tolerated. The olefin substrates with seven- or eight-membered ring **10-1s** resulted in similarly remarkable yields and regioselectivity. The exocyclic olefin **1n** bearing an additional substituent at the α-position of the double bond was also a suitable substrate for this transformation, which afforded a single isomer **2n** in 90% isolated yield. In contrast, much worse regioselectivity (**2**:**3** = 2:1 or 1:1) was obtained under classic acid promoted olefin isomerization conditions for the reaction of **1e**, **1g**, **1h** and **1m**, clearly revealing that the cobalt-catalyzed olefin isomerization was under kinetic control. Notably, the isomerization of 1,1-disubstituted acyclic olefin substrates **1t**, **1u** and **1v** proceeded in high regioselectivity as well. These reactions led to the formation of less bulky olefin products homoallylic ether **2t**, allylic amine **2u** and [illegible], [illegible] unsaturated ester **2v** in over 90% yields, albeit the *E*/*Z* ratio of the internal olefin products could not be completely controlled. Remarkably, the thermodynamically more stable isomerization products, vinyl ether and enamine, were not observed in these transformations. These above results highlighted the superior performance of these pincer cobalt catalysts in accomplishing a precise regioselectivity control, which also revealed the pivotal role of steric factor, rather than the thermodynamic stability, in such olefin isomerizations.

Scheme 3. Substrate Scope for the Regioselective Olefin Isomerization of 1.[a]

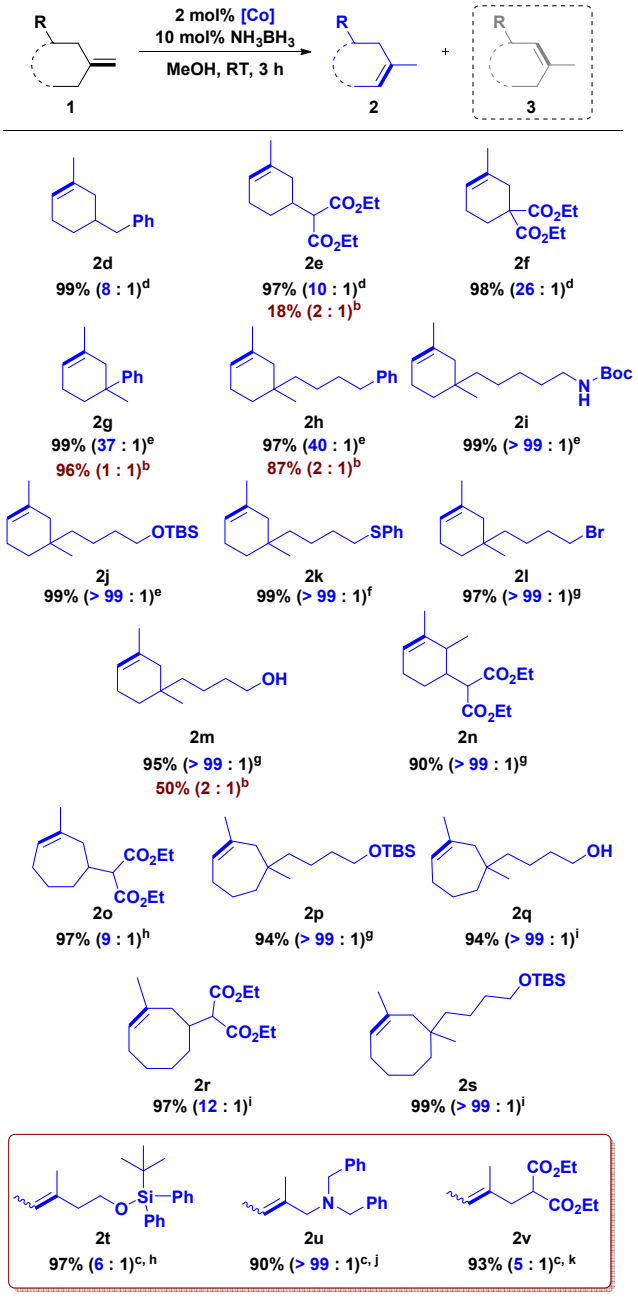

[a]>97% Conversions were achieved for all reactions. Isolated yields for a mixture of **2** and **3** were shown. The ratio of

2:3 were determined by ^{1}H NMR and shown in the parentheses. [b]The yield and regioselectivity for olefin isomerization promoted by TsOH were shown in red. [c]E/Z selectivity for **2t**, **2u** and **2v** was 2:1, 3:1 and 3:1, respectively. [d]**Co-VII** was used. [e]1 mol% **Co-IV** was used. [f]5 mol% **Co-IV** was used and the reaction temperature was 50 °C. A second portion of **Co-IV** (5 mol%) and NH_3BH_3 (10 mol%) were added into the reaction system after 3 h and the reaction was conducted for another 3 h. [g]**Co-IV** was used and the reaction temperature was 50 °C. [h]**Co-VIII** was used. [i]**Co-IV** was used. [j]0.5 mol% **Co-IV** was used and the reaction temperature was 50 °C. [k]2 mol% **Co-VI** was used and the reaction temperature was 50 °C.

The cobalt-catalyzed isomerization of γ-substituted exocyclic olefin **1w-1y** were also investigated (Scheme 4). Remarkably, the double bonds selectively monoisomerized to afford the desired isomers **2w-2y** in over 90% isolated yields. The double bond migration to the conjugated positions of 4-Ph, 4-CO_2Et and 4-NHBoc groups did not happen for all these reactions, although the corresponding conjugated olefin isomers are thermodynamically more stable. It indicated that this Co-catalyzed highly regioselective isomerization of γ-substituted exocyclic olefin was also under kinetic control.

Scheme 4. Olefin Isomerization of para-Substituted Exocyclic Olefin Substrates 1.[a]

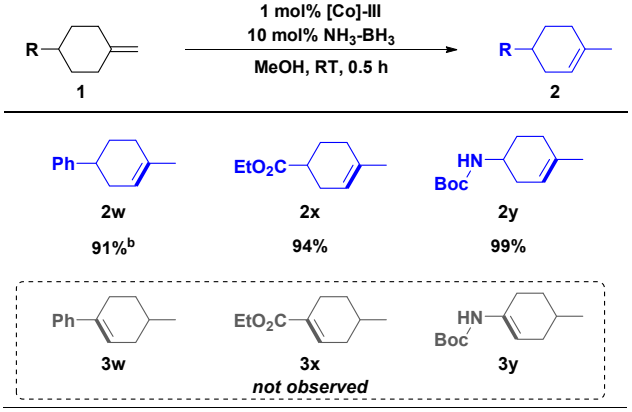

[a]Reaction conditions: 0.5 mmol substrate, 1 mol% **Co-III**, 10 mol% NH_3BH_3 in 2 mL of MeOH at RT for 0.5 h. [b]0.5 mol% **Co-III** and 5 mol% NH_3BH_3 were used.

To further demonstrate the synthetic utility of this regioselective olefin isomerization reaction, we performed a derivatization of a steroid hormone, testosterone (Scheme 5). A functionalized exocyclic olefin **1z** could be easily prepared from testosterone in two steps, including a Pd-catalyzed transfer hydrogenation and a Wittig reaction step. The regioselective olefin isomerization of **1z** could be achieved with full conversion in the presence of 4 mol% of cobalt catalyst **IV**. 87% isolated yield for a mixture of isomerized products **2z** and **3z** was attained in 3:1 regioselectivity. The isolation of the major product **2z** in high purity could be realized by preparative HPLC.

Scheme 5. Derivatization of Testosterone.

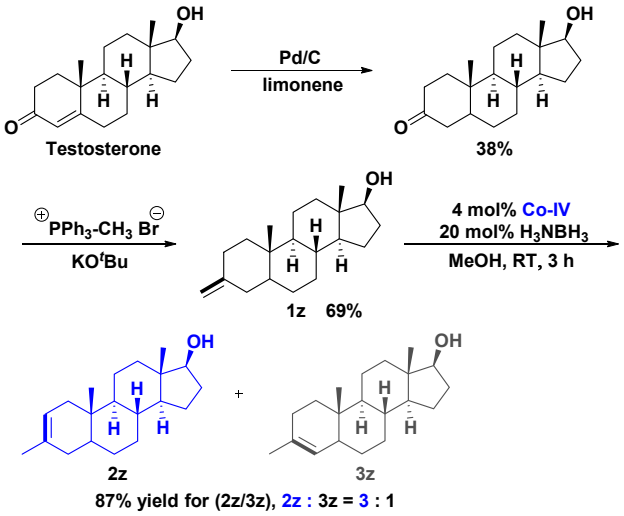

Designed Strategy for Monoisomerization

Selective monoisomerization of 1-alkenes to 2-alkenes is also a challenging kinetically controlled transformation as shown in Figure 1c. According to those informative results discussed above, we designed a new strategy for monoisomerization of 1-alkenes (Scheme 6). Knowing the fact that the substituent on β-positon of the double bond could effectively inhibit the olefin migration to the more sterically hindered side of the 1,1-disubstituted olefins, we expect to turn off the isomerization process by simply installing a substituent **R** on the β-position of 1-alkene (Scheme 6, eq. 2). In contrast, selective monoisomerization of 1-alkenes to 2-alkenes could be turned on when an **R** group is installed at the γ position of double bond (Scheme 6, eq. 3). In this case, the R group would be in the β-position of the resulting monoisomerized product 2-alkene, which would prevent further olefin migration to other internal positions. To verify this hypothesis, a series of control experiments were implemented. In fact, this cobalt catalytic system was effective for the chain walking reaction of 6-phenyl-1-hexene **4a**, affording the most stable conjugated olefin product **5a** in 78% yield and 100% conversion, in which other olefin isomers were also produced (Scheme 6, eq. 1). However, much lower conversion was indeed obtained under the same reaction conditions for the isomerization of β-siloxy-1-alkene **6** along with the generation of reduced alkane product (Scheme 6, eq. 2). Furthermore, the monoisomerization of γ-substituted 1-alkenes was investigated. Compound **8a**, γ-Hydroxyl-7-phenyl-1-heptene, was selected as the model substrate for the monoisomerization reaction. Normally this compound can be easily converted into the more stable isomerized ketone product since the hydroxyl group is an efficient directing group for chain walking reaction. After a systematic survey of pincer cobalt catalysts, we found that the selectivity of this reaction was enhanced by increasing the steric hindrance of the ligand and the most bulky catalyst **IX** gave the best result (94% isolated yield) for the monoisomerized 2-alkene **9a**. It is noteworthy that other isomerization products were not observed under these

reaction conditions. These results implied that the R group could indeed act as a switch to control the process of 1-alkene isomerization with the assistance of cobalt catalysts.

Scheme 6. A Designed Strategy for Monoisomerization of 1-Alkenes to 2-Alkenes

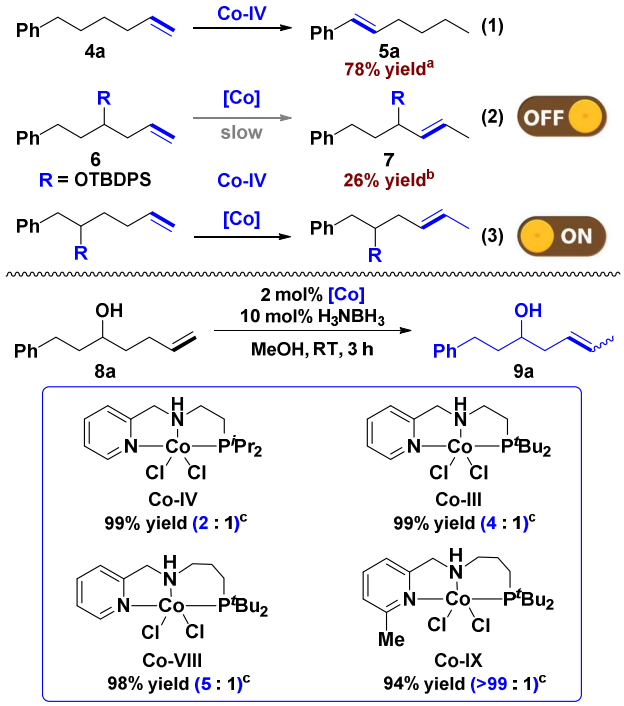

[a]The yield of 5a was determined by GC using biphenyl as internal standard. [b]The yield of 7 was determined by ^{1}H NMR and the reduced alkane product was also obtained in 13% yield. [c]The ratio of **9a** : **other isomerization products** were determined by ^{1}H NMR and shown in the parentheses.

The scope for the selective monoisomerization of γ-substituted 1-alkenes **8** to 2-alkenes **9** were investigated (Scheme 7). Over 90% isolated yields for 2-alkene products (a mixture of E/Z isomers) were obtained for all the tested substrates (**9a**-**9g**). Notably, there were no over-isomerized internal olefins observed. The substituted group R on the γ-position of double bonds could be diversified, including hydroxyl, bromo, *tert*-butyldiphenylsiloxy (OTBDPS), methyl group and even fluro group. These results demonstrated the excellency in regioselectivity and generality of this novel strategy for the monoisomerization of 1-alkenes.

Moreover, the installing of R group on the γ position, along with the uniqueness of kinetic control ability of our catalytic systems, further enables challenging *site-selective* monoisomerization of diene substrate. When diene substrate **8h** was subjected to the optimized condition, we observed only the predicted isomerization of terminal double bond (eq. 2). This result is in contrast to a similar substrate previously reported by Norton and coworkers, where the isomerization occurred on the 1,1-disubstituted double bond to form a thermodynamically more stable product.[13]

Scheme 7. Cobalt-Catalyzed Monoisomerization of γ-Substituted 1-Alkenes 8 to 2-Alkenes 9. [a]

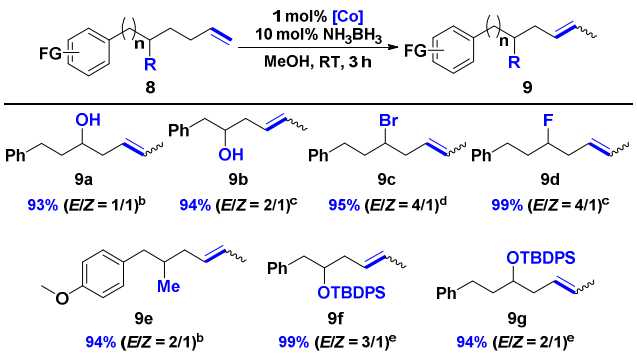

[a]Reaction conditions: 0.125 mmol substrate, 1 mol% **[Co]**, 10 mol% NH_3BH_3 in 0.5 mL of MeOH at RT for 3 h. [b]**Co-IX** was used. [c]**Co-VIII** was used. [d]2 mol% **Co-VIII** was used. [e]2 mol% **Co-IV** was used.

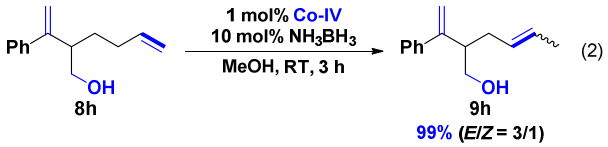

Mechanistic Studies

In general, there are mainly three possible reaction mechanisms for transition metal-catalyzed olefin isomerization process (Scheme 8).[3b] **1)** The insertion/elimination mechanism starts with a metal-hydride species possessing a free coordination site. The coordination of olefin substrate to the metal center and the following insertion of double bond into the M-H bond gives the key alkyl-metal intermediate, which undergoes the subsequent β-hydride elimination to generate the isomerized olefin product (Scheme 8, eq. 1).[3d] **2)** The π-allyl metal mechanism may proceed through either inner-sphere or outer-sphere hydrogen transfer process. The inner-sphere mechanism is initiated by an oxidative addition of the low valent metal with C-H bond in the allylic position to generate π-allyl metal-hydride complex. The following reductive elimination taking place on the other site furnishes with the olefin isomer (Scheme 8, eq. 2, up).[14] Alternatively, in the outer-sphere mechanistic pathway the ligand acts as a base to deprotonate the allylic position, leading to the formation of a π-allyl metal complex. This key intermediate gives the isomerization product after rotation over the allyl bond and the subsequent reprotonation of the M-C bond (Scheme 8, eq. 2, down).[3j] **3)** The hydrogen atom transfer (HAT) mechanism proceeded by initial HAT from a metal-hydride complex to the alkene substrate, which provided a carbon-centered radical and a metalloradical species M• with a reduced valence.[15] Finally, removal of H• from alkyl radical by M• affords the isomerized olefin and regenerates the meta-hydride species (Scheme 8, eq. 3).[11]

Scheme 8. Different Mechanisms for Transition-Metal-Catalyzed Olefin Isomerization.

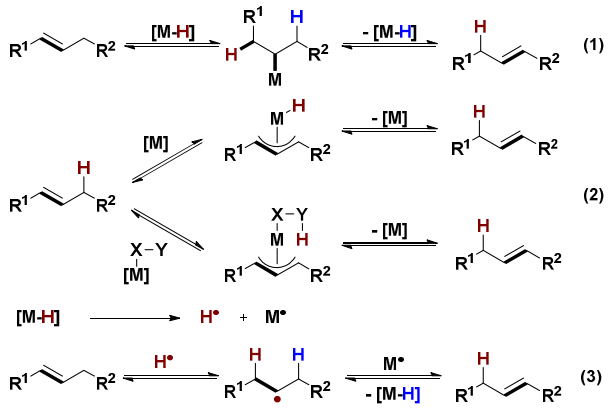

A series of control experiments were carried out to distinguish these mechanistic pathways. A mixture of **D_4-1h** containing ortho- CD_2 and the non-deuterated substrate **1m** was treated under the standard isomerization reaction conditions (Scheme 9). The isomerized products generated from this scrambling experiment were isolated and analyzed by ^{1}H NMR. The isomerization products derived from **D_4-1h** displayed a decreased deuterium incorporation, while the allylic position of isomerized product **10b** was partially deuterated. This result excluded an intramolecular 1,3-hydrogen shift reaction pathway via the π-allyl metal mechanism.

Scheme 9. Scrambling Deuterium-Labeling Experiment.

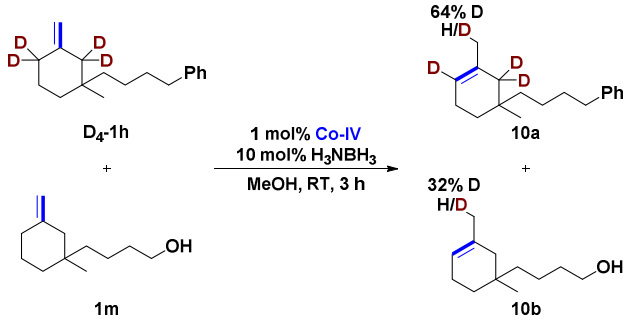

The reactions of **1j** with different radical scavengers, 1,1-diphenyl ethene, ditert-butylhydroxytoluene and 9,10-dihydroanthracene, were further examined (Scheme 10, up). There was no influence in the presence of one equivalent of these radical inhibitors. Furthermore, a radical clock reaction was designed using 1,6-diene **11a** as substrate (Scheme 10, down). If this reaction followed the HAT mechanism, phenyl substituted 5-hexenyl radical **13a** would be generated, which could undergo a very fast cyclization to produce a cycloisomerization product **15a**.[13,16] In fact, the cyclization product was not obtained under these standard reaction conditions. These results demonstrated that the HAT mechanistic pathway was very unlikely.

Scheme 10. Radical Trap Experiments.

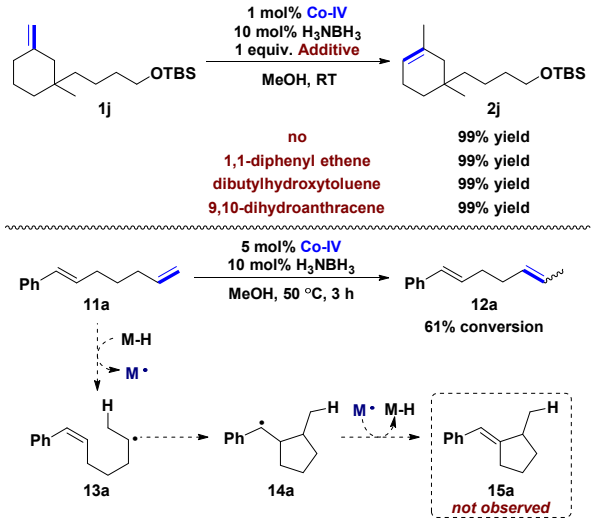

In view of the above experimental observations, we proposed an insertion/elimination mechanism for this cobalt-catalyzed olefin isomerization reaction (Figure 2). The catalytic cycle started with the coordination of **1** to cobalt(I) hydride complex **A**, which could be generated by reducing the cobalt dichloride complex using ammonia borane.[9b] Chirik and co-workers synthesized an analogous pincer cobalt (I) hydride complex by treating the (PNP)$CoCl_2$ complex with $NaHBEt_3$, which supports the reliability of such a cobalt hydride species.[17] The insertion of double bond into the Co-H bond gave the alkyl cobalt intermediate **C**. The following β-hydride elimination of H_a or H_b would lead the formation of isomerized olefin products **2** or **3**. The applied pincer cobalt catalyst could precisely differentiate the steric hindrance of reaction sites **a** and **b** due to the existence of R- substituted group, which determined the excellent regioselectivity of this isomerization process via kinetic control.

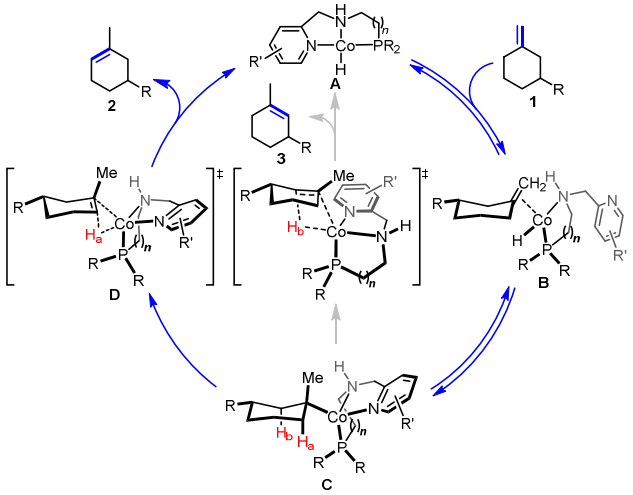

Figure 2. Proposed reaction mechanism.

DFT Computational Study

In order to elucidate the role of the NNP-Co based catalytic system in the kinetic control of olefin isomerization more comprehensively, we performed DFT computational studies employing the isomerization reaction cata-

lyzed by complex **Co-IV**. We have previously studied the mechanism of transfer hydrogenation reaction of alkynes and the isomerization of the corresponding alkene product catalyzed by the same series of NNP-Co pincer complexes, and the results revealed that the spin states of Co-containing intermediates and transition structures were triplet rather than singlet, and there is no change in spin state along the reaction pathways.[18] Therefore, in the present study the reaction mechanism is discussed on the basis of the triplet potential energy surfaces.

Because exocyclic olefins served as major type of representative substrates in this study, we first studied the isomerization mechanism of olefin **1g**. As revealed by DFT calculation, for exocyclic alkene **1g**, the isomerization to its endocyclic isomers **2g** and **3g** is thermodynamically favorable, with **2g** being more stable by 0.6 kcal/mol in terms of Gibbs free energy (Figure 3). Therefore, the isomerization under thermodynamic control would produce a mixture of **2g** and **3g** with a low selectivity, which is in agreement with the observed product distribution in Brønsted-acid-catalyzed isomerization of **1g** (see Scheme 3).

The potential energy surface of the Co-catalyzed isomerization of **1g** is shown in Figure 3. Cobalt(I) hydride complex **IN1**, derived from **Co-IV** under the reaction conditions, coordinates with exocyclic alkene **1g** to form complex **IN2**. The coordination step is endergonic by 9.1 kcal/mol, which forms a tetracoordinated cobalt(I) center with the dissociation of the pyridine ligand, in agreement with the proposed hemilabile NNP ligand design. The subsequent insertion of the exocyclic C=C bond into the Co-H bond takes place via **TS1** with an activation Gibbs free energy of 23.7 kcal/mol. The insertion step affords alkylcobalt(I) species **IN3**, and the transformation from **IN1** to **IN3** is slightly endergonic (by 4.6 kcal/mol) from **IN1**. In intermediate **IN3**, there are two sites, H_a and H_b, accessible for β-hydride elimination, where H_b site is in a close proximity to the quaternary carbon and is more hindered. DFT calculation indicated that, β-hydride elimination from H_a (via **TS2a**) is indeed more favorable than from H_b (via **TS2b**), and thus leading to the preferred isomerization product **2g** ($\Delta\Delta G^{\ddagger}$ = 1.0 kcal/mol)**.**[19] Analysis of the two transition states shows that, in **TS2b** the coordinating pyridine unit has a repulsion interaction with the phenyl group attached to the quaternary carbon (the distance between the pyridine α-CH and the phenyl CH is 2.65 Å), while such interaction is absent in **TS2a**, because the reaction center is distal to the quaternary carbon. It is notable that both β-hydride elimination pathways require higher activation barriers than the first insertion step, indicating that the insertion step is reversible, while the β-hydride elimination step is irreversible and rate-determining. After β-hydride elimination, the formed olefin-Co(I) hydride complexes, **IN4a** and **IN4b**, undergo olefin dissociation to deliver the isomerized product and release the Co(I) hydride **IN1**. The computed potential energy surface exemplified the proposed scenario of kinetic control shown in Figure 1d, though the kinetically preferred product is also thermodynamically more stable.

Given that enolates and enamines are thermodynamically more favorable compared with other alkene isomers, we sought to investigate the isomerization of alkene **1u** as another representative model, where complete kinetic control dictated the regioselectivity and thermodynamically disfavored alkene isomer **2u** was produced as the sole product (Scheme 3). Our computational result confirmed that the isomerization of **1u** to enamine **3u** is thermodynamically more favorable than to allylic amine **2u** by 0.6 kcal/mol in terms of Gibbs free energy (Figure 4). The isomerization pathway is similar to that of olefin **1g**. After coordination to Co-H complex **IN1** and alkene insertion, substrate **1u** was transformed to **IN6**, from which two different β-hydride elimination transition states lead to two regioisomers **2u** and **3u**, respectively. Hydride elimination from the methylene moiety of the ethyl group via **TS4a** requires 20.0 kcal/mol activation energy, while hydride elimination from the methylene adjacent to the amine group via **TS4b** requires 23.6 kcal/mol (starting from intermediate **IN6**).[19] Analysis of these transition structures revealed that **TS4b** involves more steric repulsions between the isopropyl groups on the phosphorus atom and the *N*-benzyl group, because the reaction center is close to the bulky NBn_2 substituent. In the favored transition structure **TS4a**, the reaction center is distal to the bulky part of the molecule and thus with much less steric repulsion. After β-hydride elimination, olefin-Co(I) hydride complexes **IN7a** and **IN7b** are generated, and olefin dissociation occurs to deliver the isomerized product as well as release the Co(I) hydride **IN1**. In this case, the steric interaction in the hydride elimination process, rather than the thermodynamic stability of the isomerization products, predominate the regioselectivity, which nicely showcased the catalyst-enabled kinetic control of olefin isomerization.

For both substrates under study, the Co-catalyzed olefin isomerization is under kinetic control, despite that exocyclic and acyclic olefin substrates exhibit different reactivities and steric control factors. The selectivity is dictated by the relative activation free energy of the two regiomeric β-hydride elimination transition states, rather than the relative thermodynamic energy of the two products. By employing carefully designed NNP-Co complexes as catalysts, the isomerization pathway with less steric hindrance would be more favorable, as exemplified above.

CONCLUSIONS

We have demonstrated a kinetically-controlled regioselective olefin isomerization reaction catalyzed by a series of well-defined cobalt complexes. Ammonia borane was used as a bench stable and mild reagent to activate cobalt catalyst precursors. The current catalytic system operates under mild conditions and allows for the isomerization of a variety of 1,1-disubstituted olefins and γ-substituted 1-alkenes with good yields and regioselectivity. Notably, by applying this protocol we enabled the efficient preparation of a key intermediate towards the total synthesis of minfiensine and a convenient derivatization of testosterone. A combined experimental and theoretical mecha-

nistic studies uncovered an insertion/elimination reaction pathway and the mechanism for regioselectivity control. We believe this strategy for the regioselective olefin isomerization via kinetic control would provide useful insights for the development of other types of practical olefin isomerization processes.

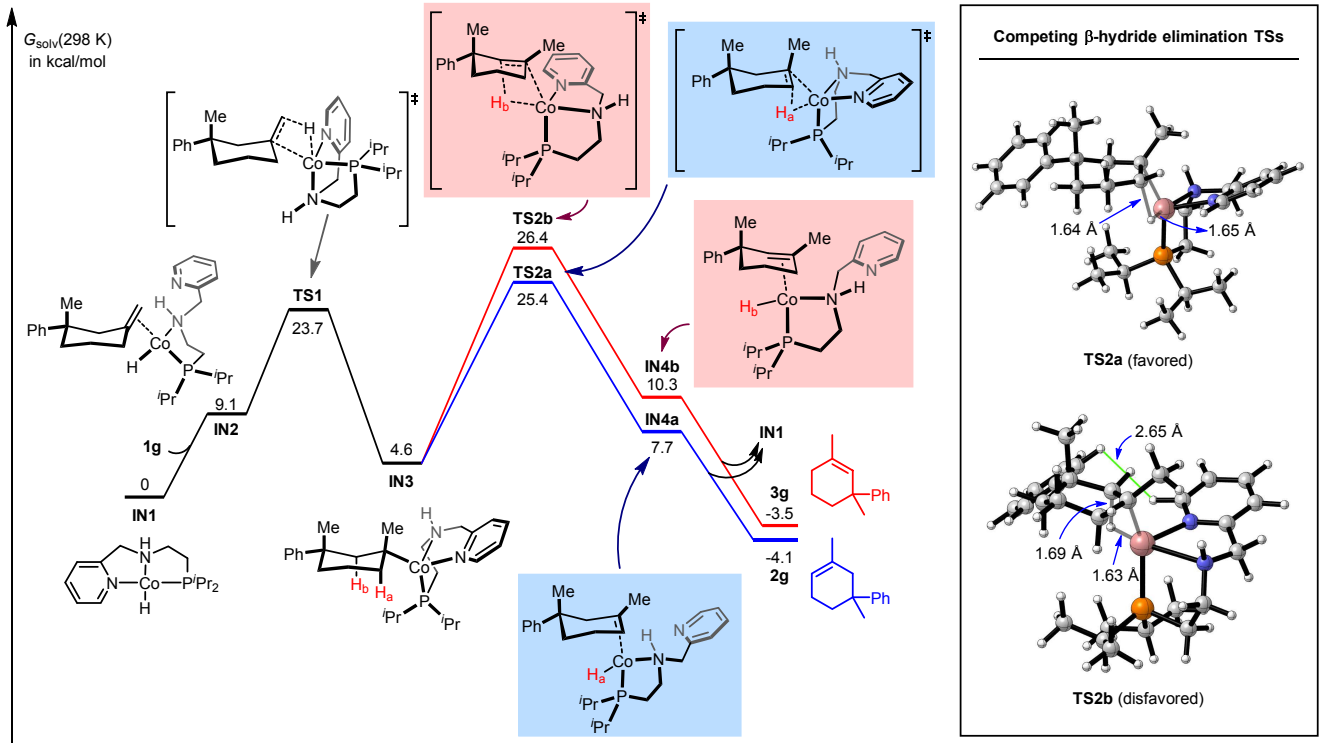

Figure 3. Potential energy surface for the Co-catalyzed isomerization of exocyclic olefin 1g.

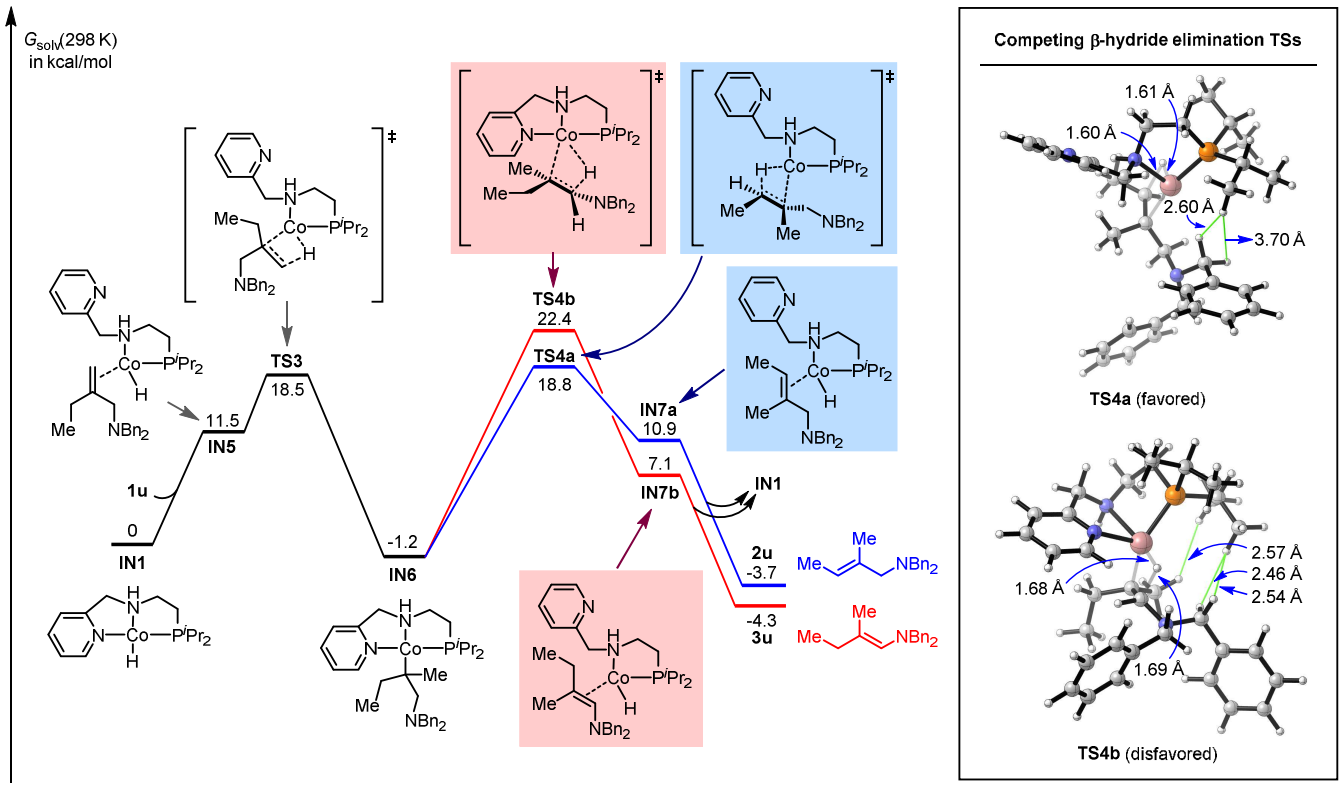

Figure 4. Potential energy surface for the Co-catalyzed isomerization of acyclic olefin 1u.

ASSOCIATED CONTENT

The Supporting Information is available free of charge on the ACS Publications website. Experimental details, Spectra and crystallographic data were included.

AUTHOR INFORMATION

Corresponding Author

*qiang_liu@mail.tsinghua.edu.cn.
*leijiao@mail.tsinghua.edu.cn.

Author Contributions

The manuscript was written through contributions of all authors. All authors have given approval to the final version of the manuscript.

Notes

The authors declare no competing financial interest.

ACKNOWLEDGMENT

This article is dedicated to Prof. Jin-Pei Cheng from CBMS of Tsinghua University on the occasion of his 70th birthday. This project was supported by the National Natural Science Foundation of China (21702118), the National Program for Thousand Young Talents of China and the 111 project. We thank Prof. Herbert Mayr from Ludwig-Maximilians-Universität München and Dr. Gang Li from Princeton University for the helpful discussions.

REFERENCES

(1) (a) Holland, P. L. *Acc. Chem. Res.* **2015**, *48*, 1696; (b) Hilt, G. *ChemCatChem* **2014**, *6*, 2484; (c) Donohoe, T. J.; O'Riordan, T. J. C.; Rosa, C. P. *Angew. Chem. Int. Ed.* **2009**, *48*, 1014.

(2) (a) Trost, B. M.; Cregg, J. J.; Quach, N. *J. Am. Chem. Soc.* **2017**, *139*, 5133; (b) Kocen, A. L.; Brookhart, M.; Daugulis, O. *Chem. Commun.* **2017**, *53*, 10010; (c) Zhuo, L.-G.; Yao, Z.-K.; Yu, Z.-X. *Org. Lett.* **2013**, *15*, 4634; (d) Mamone, P.; Grünberg, M. F.; Fromm, A.; Khan, B. A.; Gooßen, L. J. *Org. Lett.* **2012**, *14*, 3716; (e) Mayer, M.; Welther, A.; Jacobi von Wangelin, A. *ChemCatChem* **2011**, *3*, 1567.

(3) (a) Liniger, M.; Liu, Y.; Stoltz, B. M. *J. Am. Chem. Soc.* **2017**, *139*, 13944; (b) Vasseur, A.; Bruffaerts, J.; Marek, I. *Nat Chem* **2016**, *8*, 209; (c) Martínez, J. I.; Smith, J. J.; Hepburn, H. B.; Lam, H. W. *Angew. Chem. Int. Ed.* **2016**, *55*, 1108; (d) Lin, L.; Romano, C.; Mazet, C. *J. Am. Chem. Soc.* **2016**, *138*, 10344; (e) Masarwa, A.; Didier, D.; Zabrodski, T.; Schinkel, M.; Ackermann, L.; Marek, I. *Nature* **2014**, *505*, 199; (f) Larionov, E.; Lin, L.; Guénée, L.; Mazet, C. *J. Am. Chem. Soc.* **2014**, *136*, 16882; (g) Obligacion, J. V.; Chirik, P. J. *J. Am. Chem. Soc.* **2013**, *135*, 19107; (h) Werner, E. W.; Mei, T.-S.; Burckle, A. J.; Sigman, M. S. *Science* **2012**, *338*, 1455; (i) Kochi, T.; Hamasaki, T.; Aoyama, Y.; Kawasaki, J.; Kakiuchi, F. *J. Am. Chem. Soc.* **2012**, *134*, 16544; (j) Grotjahn, D. B.; Larsen, C. R.; Gustafson, J. L.; Nair, R.; Sharma, A. *J. Am. Chem. Soc.* **2007**, *129*, 9592; (k) Seayad, A.; Ahmed, M.; Klein, H.; Jackstell, R.; Gross, T.; Beller, M. *Science* **2002**, *297*, 1676; (l) Arisawa, M.; Terada, Y.; Nakagawa, M.; Nishida, A. *Angew. Chem. Int. Ed.* **2002**, *41*, 4732.

(4) Li, H.; Mazet, C. *Org. Lett.* **2013**, *15*, 6170.

(5) Pünner, F.; Schmidt, A.; Hilt, G. *Angew. Chem. Int. Ed.* **2012**, *51*, 1270.

(6) (a) Castro-Rodrigo, R.; Chakraborty, S.; Munjanja, L.; Brennessel, W. W.; Jones, W. D. *Organometallics* **2016**, *35*, 3124; (b) Perdriau, S.; Chang, M.-C.; Otten, E.; Heeres, H. J.; de Vries, J. G. *Chem. Eur. J.* **2014**, *20*, 15434; (c) Chianese, A. R.; Shaner, S. E.; Tendler, J. A.; Pudalov, D. M.; Shopov, D. Y.; Kim, D.; Rogers, S. L.; Mo, A. *Organometallics* **2012**, *31*, 7359.

(7) (a) Wang, Y.; Qin, C.; Jia, X.; Leng, X.; Huang, Z. *Angew. Chem. Int. Ed.* **2017**, *56*, 1614; (b) Schmidt, A.; Nödling, A. R.; Hilt, G. *Angew. Chem. Int. Ed.* **2015**, *54*, 801; (c) Larsen, C. R.; Erdogan, G.; Grotjahn, D. B. *J. Am. Chem. Soc.* **2014**, *136*, 1226; (d) Chen, C.; Dugan, T. R.; Brennessel, W. W.; Weix, D. J.; Holland, P. L. *J. Am. Chem. Soc.* **2014**, *136*, 945; (e) Larsen, C. R.; Grotjahn, D. B. *J. Am. Chem. Soc.* **2012**, *134*, 10357; (f) Jennerjahn, R.; Jackstell, R.; Piras, I.; Franke, R.; Jiao, H.; Bauer, M.; Beller, M. *ChemSusChem* **2012**, *5*, 734; (g) Gauthier, D.; Lindhardt, A. T.; Olsen, E. P. K.; Overgaard, J.; Skrydstrup, T. *J. Am. Chem. Soc.* **2010**, *132*, 7998; (h) Lim, H. J.; Smith, C. R.; RajanBabu, T. V. *J. Org. Chem.* **2009**, *74*, 4565; (i) Kobayashi, T.; Yorimitsu, H.; Oshima, K. *Chem. Asian J.* **2009**, *4*, 1078.

(8) Zhang, Z.-X.; Chen, S.-C.; Jiao, L. *Angew. Chem. Int. Ed.* **2016**, *55*, 8090.

(9) (a) Shao, Z.; Fu, S.; Wei, M.; Zhou, S.; Liu, Q. *Angew. Chem. Int. Ed.* **2016**, *55*, 14653; (b) Fu, S.; Chen, N.-Y.; Liu, X.; Shao, Z.; Luo, S.-P.; Liu, Q. *J. Am. Chem. Soc.* **2016**, *138*, 8588.

(10) Hanessian, S.; Giroux, S.; Larsson, A. *Org. Lett.* **2006**, *8*, 5481.

(11) Crossley, S. W. M.; Barabé, F.; Shenvi, R. A. *J. Am. Chem. Soc.* **2014**, *136*, 16788.

(12) We repeated the standard reactions reported in the literatures successfully before applying these known catalysis systems for the olefin isomerization of **1a**. See Supporting Information for more details.

(13) Li, G.; Kuo, J. L.; Han, A.; Abuyuan, J. M.; Young, L. C.; Norton, J. R.; Palmer, J. H. *J. Am. Chem. Soc.* **2016**, *138*, 7698.

(14) Sawyer, K. R.; Glascoe, E. A.; Cahoon, J. F.; Schlegel, J. P.; Harris, C. B. *Organometallics* **2008**, *27*, 4370.

(15) (a) Obradors, C.; Martinez, R. M.; Shenvi, R. A. *J. Am. Chem. Soc.* **2016**, *138*, 4962; (b) Iwasaki, K.; Wan, K. K.; Oppedisano, A.; Crossley, S. W. M.; Shenvi, R. A. *J. Am. Chem. Soc.* **2014**, *136*, 1300.

(16) (a) Li, G.; Han, A.; Pulling, M. E.; Estes, D. P.; Norton, J. R. *J. Am. Chem. Soc.* **2012**, *134*, 14662; (b) Griller, D.; Ingold, K. U. *Acc. Chem. Res.* **1980**, *13*, 317.

(17) Semproni, S. P.; Milsmann, C.; Chirik, P. J. *J. Am. Chem. Soc.* **2014**, *136*, 9211.

(18) Qi, X.; Liu, X.; Qu, L.-B.; Liu, Q.; Lan, Y. *J. Catal.* **2018**, *362*, 25.

(19) For each regiomeric β-hydride elimination pathway, multiple transition structures with different geometries have been located. The one shown in each pathway is the transition structure with the lowest Gibbs free activation energy among them. See the Supporting Inrofmation for details.

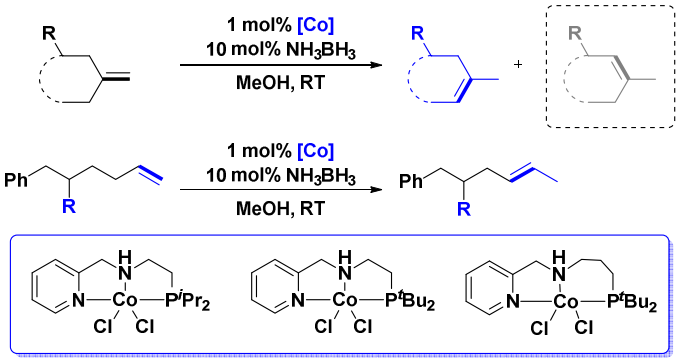
R
1 mol% [Co]
10 mol% NH3BH3
MeOH, RT
R
R
+
Ph
R
1 mol% [Co]
10 mol% NH3BH3
MeOH, RT
Ph
R
H
N
N
Co
Cl
Cl
PiPr2
H
N
N
Co
Cl
Cl
PtBu2
H
N
N
Co
Cl
Cl
PtBu2